Article

Liquid crystalline ordered collagen substrates for applications in tissue engineering

Joshua C Price, Paul Roach, and Alicia J El Haj

ACS Biomater. Sci. Eng., **Just Accepted Manuscript** • DOI: 10.1021/acsbiomaterials.6b00030 • Publication Date (Web): 03 Mar 2016

Liquid crystalline ordered collagen substrates for applications in tissue engineering

Joshua C Price[1], Paul Roach[1], Alicia J El Haj[1]*

[1]ISTM Guy Hilton Research Centre, Thornburrow drive, Stoke on Trent, ST4 7QB, UK

Email: j.price@keele.ac.uk

Key words: *Collagen; Liquid crystal; Self-assembly; Anisotropic; Tissue engineering, hMSC*

Abstract

'*This report describes methods for fabricating substrates with anisotropic order from a single solution of high concentration collagen. By exploiting the intrinsic property of collagen to behave as a cholesteric liquid crystal, we demonstrate first the production of dense collagen films containing anisotropic fibres, by simple dialysis and polymerisation in ammonia vapour. We then utilised shear driven alignment of collagen using viscous extrusion to produce aligned collagen fibres. Next, we describe an evaporation technique to observe crystalline growth into the collagen, which serves to template the substrate prior to fibrillogenesis. The ordered collagen substrates supported osteogenic differentiation of hMSCs and also oriented growth of hMSCs. We also demonstrate using Raman spectroscopy that the local protein concentration of collagen in the substrates influenced the molecular orientation of collagen, Finally, we compare the resultant textures in the substrates with section of native cornea and tendon using polarised light microscopy, which showed remarkable similarities in terms of both anisotropy and second order chiral structure. These rapid, cost effective methods could potentially serve a range of different applications in tissue engineering.*'

Introduction

The ability to generate hierarchical tissue structures *in vitro* might one day allow researchers recreate truly biomimetic cell niches in a dish. This could enable detailed study of how topographical cues within the extracellular matrix influence cell behaviour. Understanding these mechanisms could greatly improve our ability to engineer functional tissue equivalents that can be used to treat a diverse range of acute and/or pathological abnormalities. Liquid crystallinity in biopolymers such as collagen has provided scientists with inference as to the formation of anisotropic structures in tissue such as bone[1], skin[2] and cornea[3]. Observations of liquid crystallinity in collagen are typically observed in concentrations higher than 50mg/ml, far in excess of commercially available concentrations and hence limiting the ability of the researcher to readily study these interesting properties. Previous reports have successfully utilised liquid crystal phase formation in collagen to generate ordered substrates to support cell growth[4,5]. However, current methods in the literature lack the benefit of simplicity and/or standardisation that is required to permit these materials to become common place in the lab.

Furthermore, no one has yet shown distinct levels of liquid crystal phase formation from a single solution of collagen. In this report we describe three simple cost effective methods to produce aligned collagen substrates to serve broad range of tissue engineering applications. Each method is fully scalable and requires only the very basic lab equipment, allowing rapid fabrication of collagen substrates that mimic the hierarchical structure of native tissues.

Materials and methods

Substrate fabrication

2ml stock concentrations of rat tail derived collagen (9.31mg/ml, BD biosciences) were dialysed overnight against either 30% or 50% PEG-400(sigma) in 500mM acetic acid. The dialysis procedure was performed in 3ml capacity dialysis cassettes (thermos-fisher). The final concentration was estimated by volume at 50-60 mg/ml (30%PEG) and 80-90mg/ml for (50%PEG) (**Figure 1A&B**).

Method A

Method A (**Figure 1, method A)** used a 50% PEG dialysis buffer and required careful removal of the viscous collagen 'frame' from the dialysis cassette, which was then transferred to a petri dish. The petri dish was placed in an ammonia chamber (consisting of a square petri dish lines with paper towels soaked in concentrated ammonium chloride (Fisher scientific)) overnight to induce polymerisation in the substrate. The collagen frame was templated, with templates then transferred to phosphate buffered saline (PBS) in well plates and stored at 4^{o}C until ready for use.

Method B

Method B could be performed in both 30% and 50% PEG solution to dialyse the collagen. After removal of the collagen from the cassette, the frame was placed into an Eppendorf tube and heated to 50^{0}C to reduce the viscosity of the collagen. The solution was drawn into a hypodermic syringe needle (29G) and placed upright in the fridge for 30 minutes. The collagen was then extruded onto glass slides into long fibres of strongly bi-refringent collagen. The slides were placed in an ammonia chamber overnight (as before) and stored in PBS at 4^{o}C until ready for use.

Method C

Method C could be performed with either 30% or 50% PEG solution to dialyse the collagen. Solutions were heated to 50^{o}C (as before) to reduce viscosity and pipetted dropwise onto either glass coverslips or microscope slides. The solutions were covered and placed in the fridge for 30minutes before adding a neutralising buffer (equivalent 1M-HEPES) to immerse the collagen (**Figure1 method C)**. Samples were left overnight at room temperature to evaporate the immersing buffer. The

samples were then placed in the ammonium chamber for a further 4 hours before washing briefly in distilled water and subjection to 15minute UV sterilisation prior to cell seeding.

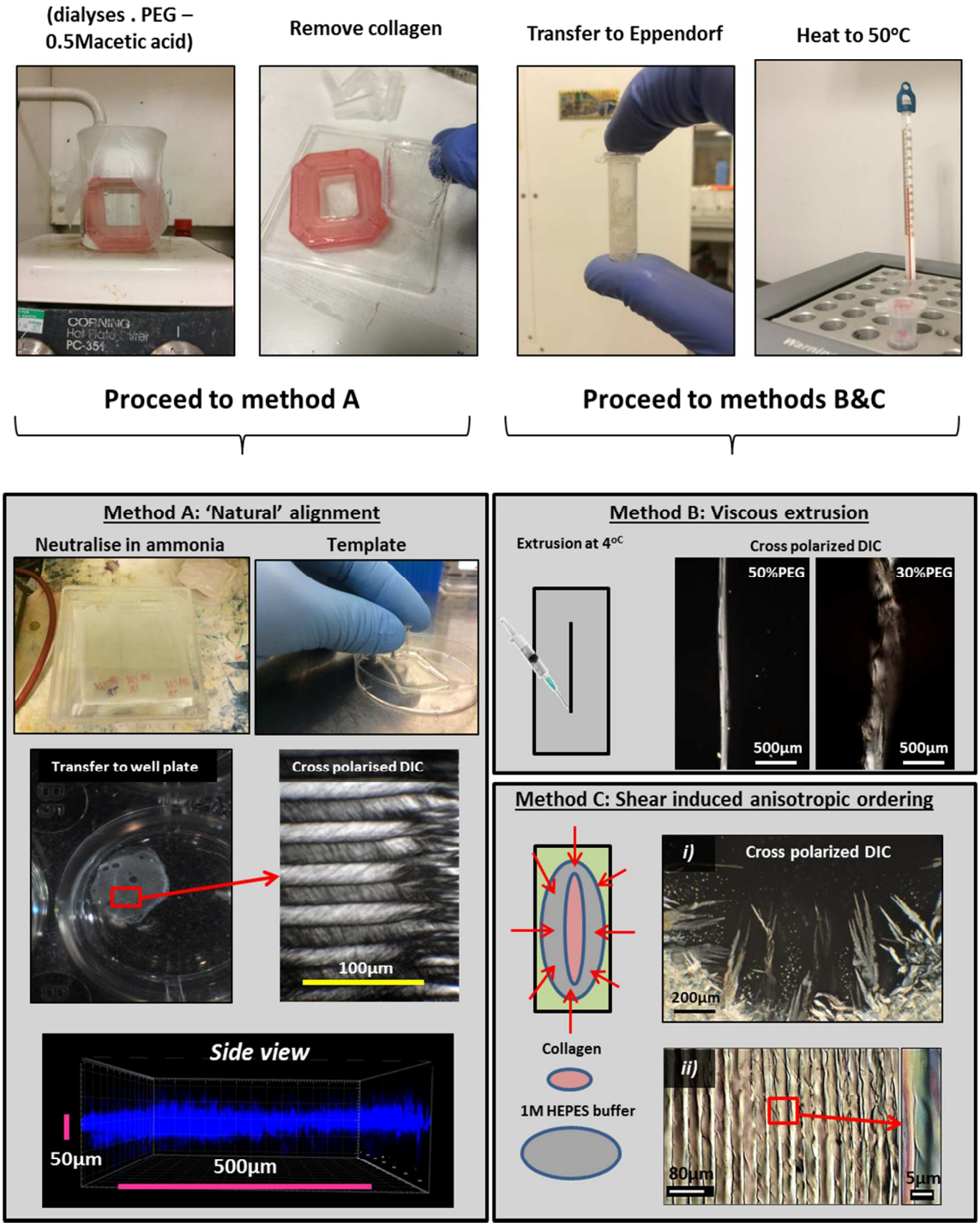

Figure 1: Fabrication of anisotropic collagen substrates from a single solution of high concentration collagen.

Cell culture

Mesenchymal stem cells were isolated via plastic adherence from a human bone marrow aspirate and maintained in cultured in proliferation media consisting of DMEM (1ng/ml glucose, w/o L-Glutamine (Lonza) containing 10% foetal calf serum (Biosera), 2% penicillin-streptomycin (Lonza), 1% Non-essential amino acids (Sigma) and 1% L-Glutamine (Lonza). Prior to seeding onto collagen substrates, cells were labelled with a PKH26 fluorescent tracker (Sigma) according to the manufacturer's instructions. For osteogenic differentiation of MSCs, cells were maintained in proliferation media supplemented with 150µg/ml ascorbic acid (Sigma), 10^{-8}M dexamethasone (Sigma) and 2mM sodium β-glycerophosphate (Sigma). Experiments were terminated by fixing samples in 10% neutrally buffered formalin (Fisher) for 15 minutes at room temperature.

Histology

After fixation, cell nuclei were stained using Harris haematoxylin solution (Sigma) for 30 seconds followed by 30 secs emersion in Scots tap water. Cell cytoplasm was stained using Eosin, immersing samples for 30 seconds followed by brief washes in DH_2O. The Von kossa method was employed to detect bone formation using 5% silver nitrate (sigma) in DH_2O. Samples were washed thoroughly in DH_2O before immersion in silver nitrate solution for 30 minutes, followed again by thorough washes in DH_2O. Samples were then exposed to 90mjoule UV irradiation for 15 minutes in a Bio rad GenX UV chamber.

Immunocytochemistry

Immunocytochemistry was performed by blocking non-specific binding using 1%BSA (Agilent) in PBS for 1 hr at room temperature. Primary antibody staining was performed overnight at 4^oC using human Osteocalcin monoclonal antibody (R&D systems) diluted to 2µg/ml in 0.1% BSA in PBS-0.1% -tween. Samples were then incubated in Alexafluora 488 or (2µg/ml, 0.1% BSA, 0.1% Tween-20 in PBS) (Abcam) for 1hr at room temperature in the dark. Nuclear staining was performed with 4', 6-diamidino-2-phenylindole (DAPI) for 15 minutes at room temperature in the dark.

Tissue sample preparation

Dissected pig cornea and chicken tendon were fixed in neutrally buffered formalin before paraffin embedding using an automated vacuum tissue processor (Kedee). 10µm sections were cut using a microtome, with sections transferred to microscope slides. Sections were then deparaffinised in xylene and rehydrated in serial ethanol dilutions in dH_2O. Sections were mounted onto slides with coverslips using DPX mounting medium (Sigma) prior to imaging.

Imaging

Confocal imaging of the samples was performed using an Olympus U-TBI 90 confocal microscope, employing either reflectance mode, or using standard fluorescence mode. Polarised light microscopy was performed using a Brunel SP300 polarising microscope. Samples were places between cross polarisers and images were captured using an inverted digital camera (Nikon). Whole mount fluorescence imaging was performed using a Leica Mz10F dissection microscope. Histologically stained samples were imaged using an EVOS® FL Colour Imaging System.

Raman spectroscopy

Raman spectra for collagen substrates fabricated using 'Method A' were taken on a DXR Raman microscope (Thermo scientific) using a 532nm laser. Raman spectral mapping was performed using an Olympus TH4-200 10x objective through a 50μm pinhole aperture. Spectra from a total of 252 points were obtained over an area of 2.6x0.8mm with a summed average of 10 spectra/point. Spectral analysis was performed using an Omnic Specta software platform.

Results

Method A

Alignment of the substrate using Method A was heterogeneous within the films. The central region of films (**Figure 1, method A)** was around 50μm thick and possessed anisotropic fibre arrangements. By contrast, the much thicker frame around the collagen films did not possess obvious anisotropic fibres, suggesting surface boundary conditions play an important role in guiding alignment. Further supporting this hypothesis was the presence of more pronounced anisotropy in regions localised to boundary conditions introduced by the formation of air bubbles **(Figure 2C&D)**. The induction of collagen alignment by stress cues was supported by observations made under polarised light in viscous solutions prior to polymerisation of the substrate in ammonia vapours. By applying a local stress cues using tweezers (**Figure2 Bi**) we observed through cross polarisers strongly birefringent patterns representing the local alignment of collagen. After the stress cue was removed, the solution returned to its original state (**Figure 2Bii)**. The substrate morphology and the comprising cells labelled with PKH26 could be monitored live in culture using confocal microscopy (**Figure 2E)**. hMSCs cultured on the substrates underwent osteogenic differentiation after 14 days culture in osteogenic media This was demonstrated by Von Kossa staining, showing the formation bone nodules on the substrate (**Figure 2F, black granules)** and by immunocytochemistry at day 14, which showed differentiating hMSCs secreting osteocalcin into the surrounding ECM (**Figure 2F inset).**

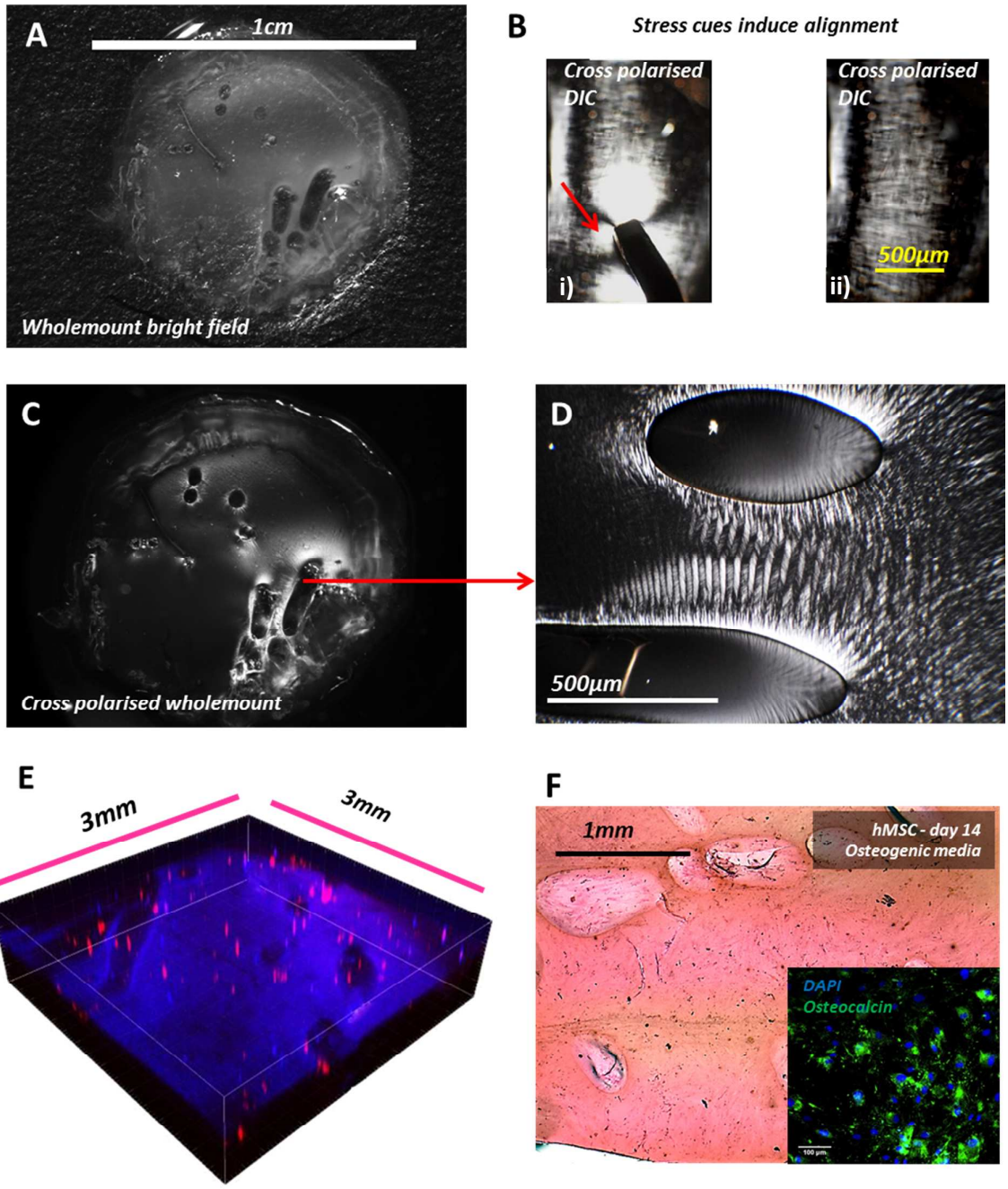

Macroscale collagen films possessing anisotropic fibre arrangements support the growth and differentiation of hMSCs. A) *Multiple templated films of collagen could be obtained from a single dialysis cassette; in this case the template yielded circular films with a 1cm diameter.* ***C****) Cross polarised imaging of high collagen concentrations in solution show typical birefringence patterns, which when subjected to stress cues* ***(Bi)*** *induces local alignment of collagen (arrow inset),Which was diminished after removal of the stress cue****(Bii)****.* ***D)*** *Birefringence in the templated films represented areas of anisotropic ordering between surface boundaries created by bubble formation during dialysis.* ***E****) Both substrate morphology (blue) and the comprising cells (red) could be monitored in live culture, and underwent osteogenic differentiation after 14 days (****F****). Black granules represent bone nodule formation and inset shows production of osteocalcin by hMSCs.*

Method B

The production of aligned collagen fibres using method B required high a collagen concentration (obtained in 50%PEG) yielding more homogeneous, birefringent fibres when compared with fibres produced using 30% PEG (**Figure 1, Method B**). After overnight exposure to ammonia vapours, hMSCs seeded onto the substrate aligned parallel to the fibre direction, which was confirmed using confocal microscopy (**Figure 3A**). Interestingly, reflectance microscopy performed 1 day after cell seeding, indicated changes in density of collagen within individual fibres. A column of dense, aligned collagen was present around the periphery of the fibres, with a reduction in density toward the centre of the fibre (**Figure 3B**). hMSCs remained adhered to the fibres across a culture period of 7 days and retained an aligned morphology parallel to the fibre direction (**Figure 3C-E**).

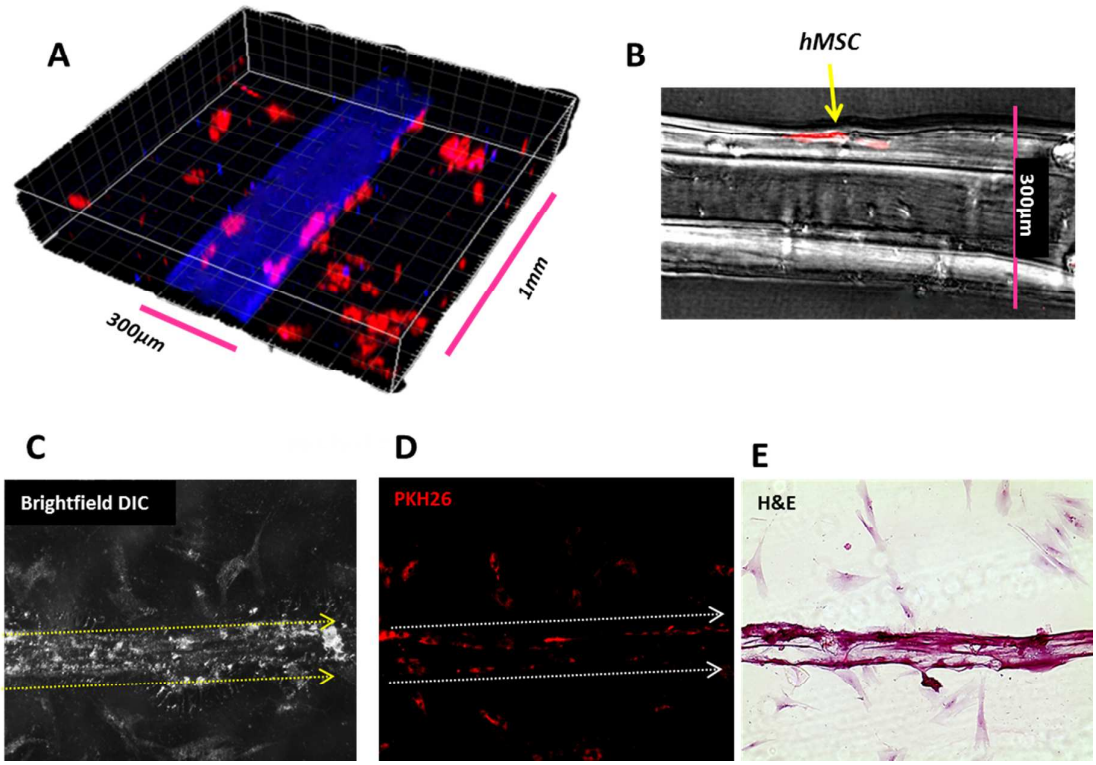

Figure 2. Production of aligned collagen fibres using viscous extrusion to support oriented growth of hMSCs. A) *Confocal imaging of the fibers day 1 after cell seeding showed adhered hMSC (red) aligned parallel to fiber direction (blue).* ***B)*** *Merged Z-stack reflectance microscopy indicated a change in fiber density between the fiber boundary and central regions of the fiber. After 7 days in culture, adhered MSCs s remained aligned in the direction of the fibers(inset arrows)* ***C,D&E).***

Method C

Method C describes a novel application using HEPES evaporation to template the collagen through crystallization (**Figure 1. Method C)**. Cross polarised imaging of the substrates after evaporation was complete, revealed a range of different orders, including regions of nested arcs (**Figure4A)** similar to that seen in lamellar bone[6], as well as areas of distinct anisotropic banding **(Figure4C)**. Temporal formation of different crystalline structures could be observed through cross polarisers, and showed rapid crystal growth across the substrate (**see supplementary video 1).** High magnification cross polarized images showed chiral nematic textures with helical pitch running orthogonal to the fibril orientation (**Figure 1, method 3, i&ii)**. During washing with distilled water, the crystalline HEPES structure rapidly dissolved (**see supplementary video 2)**, leaving behind the templated collagen underneath. Eosin staining of the substrates after fixation **(Figure4B)** showed the broad range of templated textures in the collagen due to HEPES evaporation. Higher magnification images (**Figure4D&E)** identify regions that were imaged using confocal microscopy during live culture. This enabled us to correlate the presence of oriented cells within the HEPES templated textures. hMSCs seeded onto substrates oriented themselves in the direction of banding **(Figure4F&G)** and showed no noticeable changes in viability after three days in culture.

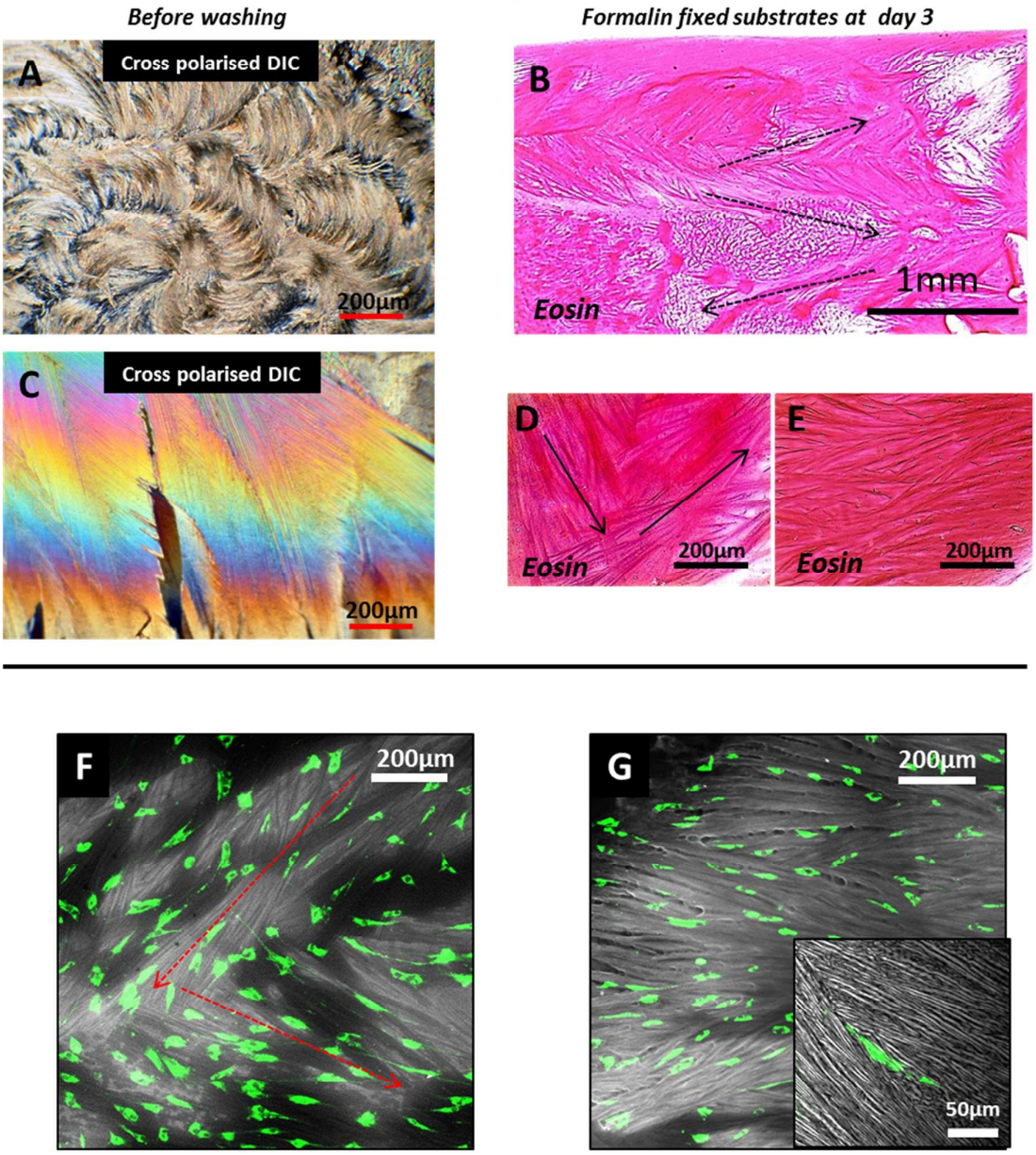

Figure 3. Evaporation of 1M HEPES buffer induces unique crystalline templates in highly concentrated collagen. (A&C) *The evaporation of 1M HEPES buffer over the substrates formed nested arc patterns as well anisotropic crystalline structures. During washing the HEPES structure rapidly dissolved (see supplementary video 2), leaving behind the templated collagen structure (**B**). Higher magnification imaging of the fixed substrates **(D&E)** identified regions that were monitored during live culture using confocal microscopy (**F&G**).*

Raman spectroscopy of naturally aligning films

Areas with prominent anisotropy in substrates produced using method A were analysed using Raman spectroscopy to assess the changes in substrate composition between regions assumed to be isotropic (random order and low birefringence) and areas containing strongly bi-refringent finger print textures (FT), assumed to be cholesteric phases of liquid crystal collagen. Spectral mapping of the 2800-3000cm^{-1} C-H stretching regions (non-specific to proteins and lipids) indicated an increase in the local concentration of collagen between isotropic and FT regions of the substrate (**Figure 5A-C**). The resulting textures in the naturally aligning films also changed according to the composition of the dialysis buffer. 50% PEG400 in 0.5Macetic acid produced workable films with distinct banded structures, yielding Raman spectra typical of signature region of collagen type 1[7]. By changing the buffer to 50% PEG35000(300mg/ml in DH_2O)[8] 0.5Macetic acid, we first observed a dramatic increase in concentration. The collagen contained within the dialysis membrane in this instance was very difficult to work with, and was removed in small quantities of film fragment. Under the polarised microscope, the films fragments exhibited a changes in texture compared with the PEG400 dialysis method, and in certain areas selectively diffracted blue light (**Figure 5D, inset pictures**) the materials associated Raman spectra also changed relative to collagen dialysed against PEG-400 (**Figure 5D, inset red boxes)**. The shoulders in the 1400-1500cm^{-1} C-H region showed a shift in the peak centre of gravity between PEG 35000 and PEG 400 dialysed substrates. In the 1440-1490 Amide III region, there were slight peak shifts, as well as changes in the peak centre of gravity. A marked peak shift was observed in the 1000-1150cm^{-1} CH_2 deformation region, with the peak centre of gravity shifting from 1135cm^{-1} and 1059cm^{-1}, to 1096 and 1031cm^{-1} respectively between PEG400 and PEG35000. Additionally, the hydroxyproline peak centre of gravity shifted from 886cm^{-1} in PEG 400 dialysed substrates to 876cm-^{1} in PEG 35000 dialysed substrates.

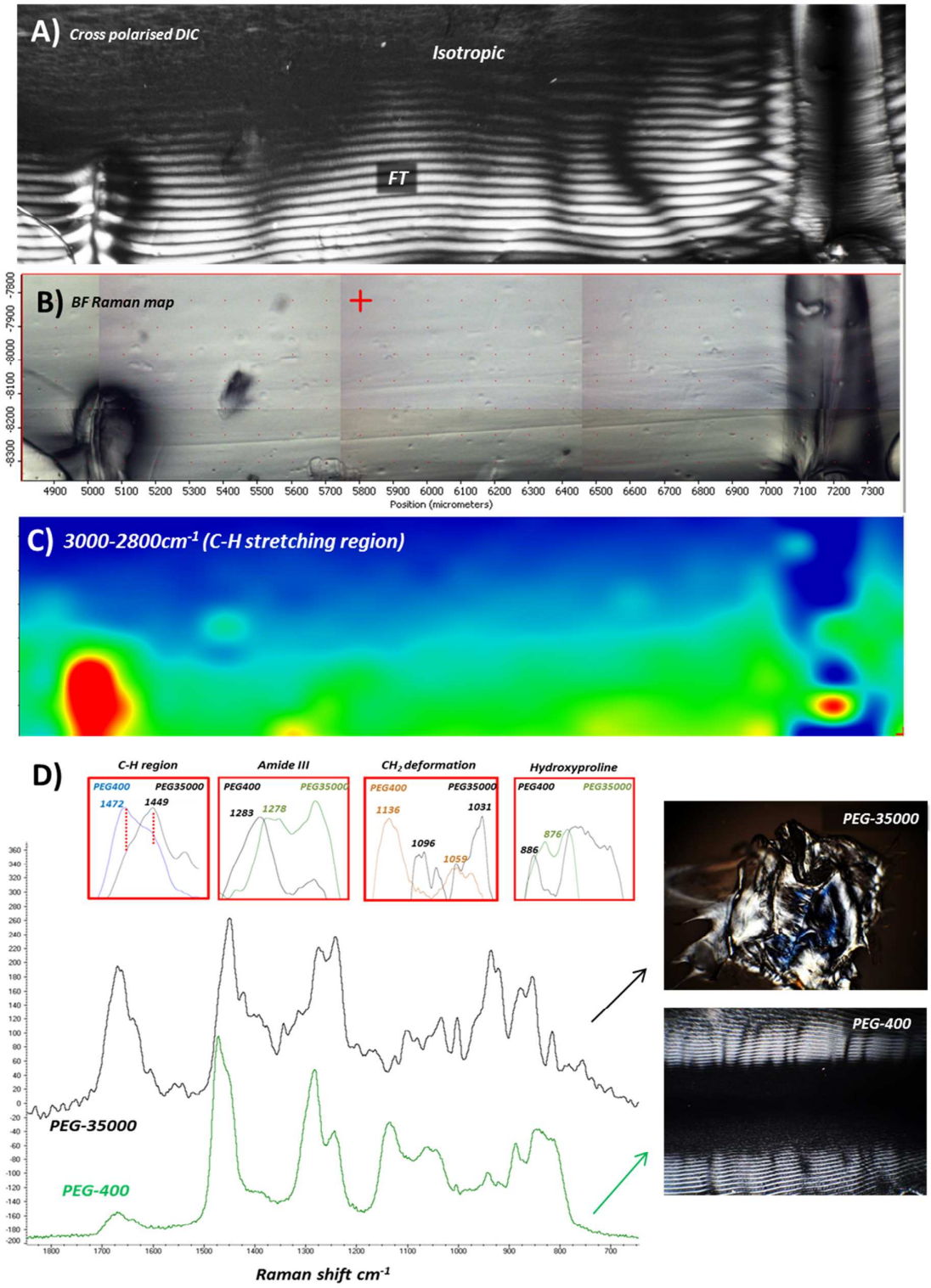

Figure 5. Raman spectroscopy of naturally aligned type 1 collagen films. A) *Cross polarised DIC of Raman mapping area showing the transition from isotropic to fingerprint textured (FT) collagen.* ***B)*** *Bright field Raman mapping area.* ***C)*** *Raman map of 3000-2800cm^{-1} C-H stretching region showing an increase in the local concentration of collagen in FT regions.* ***D)*** *Raman spectra of collagen films showing signature region for collagen type 1. Changes in Raman spectra due to dialysis against PEG35000 (top) and PEG400 (bottom) in different regions are shown in red boxes. Inset images show changes in texture under polarised light according to the corresponding Raman spectra.*

Discussion

The results described using the natural alignment method (Method A) show that the presence of topographical defects in the substrates during polymerisation produces stably aligned collagen fibres. Coupled with analysis by Raman spectroscopy, it appears that the presence of topographical defects influences the local concentration of collagen during dialysis, resulting in heterogeneously ordered films. The change in molecular orientation due to increasing concentration likely represents a lyotropic liquid crystal phase transition. Supporting this hypothesis are changes in the resultant textures of the material in different dialysis buffers, a result similarly observed by Peixoto et al. who studied in detail the changes in molecular orientation of collagen in different solvents as they undergo liquid crystal phase transitions[9].

The shifts in the Raman peaks, and also the change in the peak intensities between PEG400 and PEG35000 dialysed substrates further indicate significant structural changes in collagen assembly as the concentration is increased. The peak shifts observed in the hydroxyproline region could represent alterations in collagen triple helix stability due to a change in the bond energy of hydroxyproline residues [10]. Likewise, the prominent peak shift in the 1000-1150cm^{-1} could indicate the occurrence of a separate liquid crystal phase transition, whereby changes occur in the interaction of paraffinic side chains due to reduced water content in PEG35000 versus PEG400 substrates[11]. This hypothesis could be also supported by changes in the peak centre of gravity in the 1400-1500cm^{-1} region, indicative of paraffinic chains[12]. Deconvolution algorithms could further provide useful information on the underlying spectra which define the shoulder regions of these peaks. Collectively, the peaks shifts between the two substrates might explain the change in substrate texture under the microscope. It is reasonable to suggest that the lower concentration PEG400 system comprises of large scale anisotropic amphiphilic aggregates linked by paraffinic side chains[13], and that the more concentrated PEG35000 system, having undergone a higher order phase transition, experienced significant changes in protein conformation. The dark blue appearance of PEG35000 substrates under the microscope could indicate the presence pre-cholesteric liquid crystal blue phases. Blue phases occur in an intermediate transition of chiral liquid crystals and are characterised by their cuboidal packing structure, and ability to selectively diffract light in the visible spectrum[14]. However, critical concentrations for blue phase liquid crystals have been reported to lie in between the isotropic and cholesteric phases[14], and thus it is unclear that if this were the case, why lower concentration PEG400 substrates exhibit such prominent cholesteric banding. Despite this, our results demonstrate how useful a tool Raman spectroscopy can be when probing changes in molecular chemistry of collagen solutions as they undergo supramolecular self-assembly.

Importantly from a tissue engineering perspective, the fabrication process did not adversely affect cell behaviour in the context of osteogenic differentiation of hMSCs. Collagen type 1 constitutes the

majority of proteins found in human body, and comprises about 90% of the organic phase of bone tissue[15]. The ordered lamellar structure in bone is believed to be influenced by the formation of cholesteric phases in collagen[16]. Based on this, our results could well reflect the physiochemical process of hierarchical tissue formation under cell free *in vitro* conditions. It is unsurprising that we can differentiate hMSCs toward an osteoblastic lineage, since collagen is extensively reported to be an excellent growth substrate to promote bone formation[17,18,19]. The ability to control the orientation of collagen at the nanoscale and maintain this architecture during the culture and differentiation of stem cells might realise an important step forward in the production of biomimetic tissue equivalents. Further to this, whilst this has paper focused on the production of bone, the orientation in our naturally aligned collagen films is remarkable similar to that seen in cornea and tendon (**Figure 6)**. Further work to explore the behaviour of different cell types such as corneal stromal fibroblasts or tenocytes, could provide evidence for a range of tissue engineering applications for the collagen substrates described in this report.

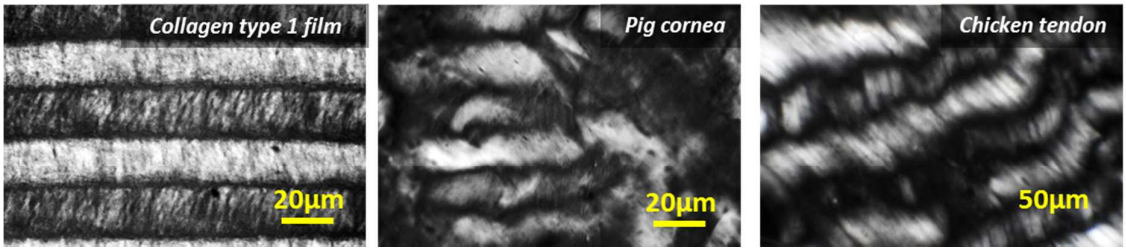

Figure 6. Cross polarised images comparing collagen orientation in type 1 collagen films, pig cornea and chicken tendon.

The results obtained using method 2 represent a simplified adaptation of methods described by Kirkwood and Fuller [4], in which a tri axial robotic arm was used to extrude 20mg/ml solutions of collagen onto slides, after which ambient desiccation further increased concentration and induced fibrillogensis. This automated fabrication method has also been further adapted to manufacture bilayer transparent films for use as corneal substitutes[20]. Our results suggest that by using a higher starting concentration of collagen we can significantly reduce the complexity of the system, making the production of these aligned fibres far more available to researchers. However it should not be understated that the use of automation presents a system with a higher rate of reproducibility, and also reflects more accurately a process controlled manufacturing platform. (**Figure 3B**) reports a novel finding, whereby alignment using narrow channel extrusion might represent electrostatic interactions between the collagen and stainless steel surface of the needle. It is reasonable to suggest the increased alignment of the collagen molecules on the fibre periphery was due to interactions with the adsorbing steel surface during dynamic flow. Li and colleagues describe a similar phenomenon in molecular

configurations of DNA in torsional flow cells, reporting changes in molecular deformation of DNA closer to an adsorbing glass surface[21]. Approaches to modelling polymer dynamics in shear flow have been reported by a number of different groups[22,23], suggesting our liquid crystalline fibre production method could provide a useful experimental platform to validate these models.

The formation of cholesteric order in HEPES/collagen substrates in method C, infers liquid crystal phase formation driven by shear force during HEPES evaporation. Chung et al reported a similar phenomenon in genetically engineered viruses using an oscillating dip coat method [24].They concluded that shear force was responsible for driving aligned fibril formation with chiral nematic helical axis aligned orthogonal to the fibril direction. Our results might reflect a system where shear stress, induced by crystalline HEPES, orients the collagen molecules; however at this stage we do not have precise control of the collagen/HEPES system. It is reasonable to postulate that liquid crystal director growth in our collagen system could be controlled through specific environmental factors such as temperature, humidity or pressure. Further to this, it would be interesting to test the effects of different buffers on the resultant properties of the substrate, such as for example stiffness or optical transparency.

The use of dialysis membranes to induce LC behaviour in collagen is widely established in the literature. Similar to our system, Saidi et al. used dialysis membranes to concentrate collagen solutions above the critical concentration required for liquid crystal self assembly[25]. They then neutralised the solution using PEG titration and spatially confined the solutions between coverslips to induce aligned fibre formation during fibrillogenesis [25]. Interestingly whilst this study was able to produce aligned collagen substrates, they did not report higher order chiral structures running orthogonal to the axis of anisotropy. Furthermore, we could argue that similar to the comparison of method made with Kirkwood and Fuller, that our procedure represents a simpler and more widely available technique. Coupled with this, since the alignment procedure described in Method A is performed in the dialysis cassettes and not using coverslips, it is easily scalable due to the dialysis cassettes being commercially available in a range of different sizes. Interestingly, the formation of a chiral axis in the substrates in method A was highly sensitive to the initial volume of collagen in the dialysis cassette, indicating that the alignment process is dependent on the degree of confinement during self-assembly.

Alignment of collagen using dialysis has also been achieved via incorporation of nanocrystalline cellulose into concentrated collagen solutions [26] and in high concentration collagen type III using a using a carbodiimide based chemistry technique [27]. Whilst alignment of collagen type IV using similar procedures has not to our knowledge been investigated, it is not unreasonable to suggest that alignment is achievable using these methods, particularly if we take into account early reports of liquid crystalline phases in collagen type IV extracted from bovine anterior lens capsules[28].

Based on existing evidence, together with recent theoretical models indicating that liquid crystalline behaviour can accurately describe experimental assemble patterns of collagen[29], it is surprising that these methods has not yet become routine in the field of tissue engineering. This may be in part due to the diverse and often complex set of protocols that are described to manufacture workable collagen substrates containing hierarchical assemblies. Utilising the available literature on collagen alignment to develop simple, rapid and cost effective protocols could make the use of self-assembled hierarchically ordered substrates far more available to tissue engineers. Further to this, the field of vibrational spectroscopy will no doubt benefit from low cost, reliable experimental systems, which can accurately relate nanoscale alterations in protein conformation to changes in material properties.

Conclusion

In conclusion, by applying a broad range of basic laboratory techniques, we demonstrate remarkable versatility in this commonly used and widely available biomaterial. Using Raman spectroscopy we have also observed nanoscale conformational changes in protein structure that may represent distinct liquid crystal phase transitions in collagen. The need for simple and cost effective fabrication of biomimetic materials will be important in realising clinically relevant regenerative medicine therapies. As well as this, a deeper understanding of the physical processes that govern anisotropic ordering in biopolymers could greatly improve our ability to engineer materials that mimic the hierarchical structure of native tissues.

Acknowledgements

The authors would like to acknowledge Dr Yvonne Reinwald and Ms Rachel Gater for providing samples of tendon and cornea. The authors would also like to thank Dr Damien McDonnel for his insightful discussions on liquid crystalline behaviour and ongoing encouragement with this work.

Supporting Information Available

The following files are available free of charge: Supplementary video 1 shows the growth of crystalline structures during evaporation of HEPES of over viscous solutions of collagen. Supplementary video 2 shows HEPES crystalline structure dissolving during washing, following crystalline templating procedure.

Funding sources

EPSRC DTC in Regenerative medicine, Keele University. Grant funding number: EP/F500491/1

References

(1) Giraud Guille, M. M.; Mosser, G.; Helary, C.; Eglin, D. Bone Matrix like Assemblies of Collagen: From Liquid Crystals to Gels and Biomimetic Materials. *Micron* **2005**, *36*, 602–608.

(2) Giraud-Guille, M. M.; Besseau, L.; Chopin, C.; Durand, P.; Herbage, D. Structural Aspects of Fish Skin Collagen Which Forms Ordered Arrays via Liquid Crystalline States. *Biomaterials* **2000**, *21*, 899–906.

(3) De Sa Peixoto, P.; Deniset-Besseau, A.; Schmutz, M.; Anglo, A.; Illoul, C.; Schanne-Klein, M.-C.; Mosser, G. Achievement of Cornea-like Organizations in Dense Collagen I Solutions: Clues to the Physico-Chemistry of Cornea Morphogenesis. *Soft Matter* **2013**, *9*, 11241.

(4) Kirkwood, J.; Fuller, G. Liquid Crystalline Collagen: A Self-Assembled Morphology for the Orientation of Mammalian Cells. *Langmuir* **2009**, *25*, 3200–3206.

(5) Tang, M.; Ding, S.; Min, X.; Jiao, Y.; Li, L.; Li, H.; Zhou, C. Collagen Films with Stabilized Liquid Crystalline Phases and Concerns on Osteoblast Behaviors. *Mater. Sci. Eng. C* **2016**, *58*, 977–985.

(6) Sanchez, C.; Arribart, H.; Guille, M. M. G. Biomimetism and Bioinspiration as Tools for the Design of Innovative Materials and Systems. *Nat. Mater.* **2005**, *4*, 277–288.

(7) Júnior, Z. S. S.; Botta, S. B.; Ana, P. A.; França, C. M.; Fernandes, K. P. S.; Mesquita-Ferrari, R. A.; Deana, A.; Bussadori, S. K. Effect of Papain-Based Gel on Type I Collagen - Spectroscopy Applied for Microstructural Analysis. *Sci. Rep.* **2015**, *5*, 11448.

(8) Nudelman, F.; Pieterse, K.; George, A.; Bomans, P. H. H.; Friedrich, H.; Brylka, L. J.; Hilbers, P. a J.; de With, G.; Sommerdijk, N. a J. M. The Role of Collagen in Bone Apatite Formation in the Presence of Hydroxyapatite Nucleation Inhibitors. *Nat. Mater.* **2010**, *9*, 1004–1009.

(9) De Sa Peixoto, P.; Deniset-Besseau, A.; Schanne-Klein, M.-C.; Mosser, G. Quantitative Assessment of Collagen I Liquid Crystal Organizations: Role of Ionic Force and Acidic Solvent, and Evidence of New Phases. *Soft Matter* **2011**, *7*, 11203.

(10) Kotch, F. W.; Guzei, I. A.; Raines, R. T. Stabilization of the Collagen Triple Helix by O-Methylation of Hydroxyproline Residues. *J. Am. Chem. Soc.* **2008**, *130*, 2952–2953.

(11) Lippert, J. L.; Peticolas, W. L. Laser Raman Investigation of the Effect of Cholesterol on Conformational Changes in Dipalmitoyl Lecithin Multilayers. *Proc. Natl. Acad. Sci. U. S. A.* **1971**, *68*, 1572–1576.

(12) Talari, A. C. S.; Movasaghi, Z.; Rehman, S.; Rehman, I. ur. Raman Spectroscopy of Biological Tissues. *Appl. Spectrosc. Rev.* **2015**, *50*, 46–111.

(13) Neto, A. M. F.; Salinas, S. R. a. The Physics of Lyotropic Liquid Crystals: Phase Transitions and Structural Properties. In *The Physics of Lyotropic Liquid Crystals: phase transitions and structural properties*; Oxford University Press, 2005; p. 5.

(14) Seideman, T. The Liquid-Crystalline Blue Phases. *Reports Prog. Phys.* **1999**, *53*, 659–706.

(15) Hadjidakis, D. J.; Androulakis, I. I. Bone Remodeling. *Ann. N. Y. Acad. Sci.* **2006**, *1092*, 385–396.

(16) Giraud-Guille, M.-M.; Besseau, L.; Martin, R. Liquid Crystalline Assemblies of Collagen in Bone and in Vitro Systems. *J Biomech* **2003**, *36*, 1571–1579.

(17) Ignatius, a; Blessing, H.; Liedert, a; Schmidt, C.; Neidlinger-Wilke, C.; Kaspar, D.; Friemert, B.; Claes, L. Tissue Engineering of Bone: Effects of Mechanical Strain on Osteoblastic Cells in Type I Collagen Matrices. *Biomaterials* **2005**, *26*, 311–318.

(18) Parreno, J.; Buckley-Herd, G.; De-Hemptinne, I.; Hart, D. a. Osteoblastic MG-63 Cell Differentiation, Contraction, and mRNA Expression in Stress-Relaxed 3D Collagen I Gels.

Mol. Cell. Biochem. **2008**, *317*, 21–32.

(19) Serpooshan, V.; Julien, M.; Nguyen, O.; Wang, H.; Li, A.; Muja, N.; Henderson, J. E.; Nazhat, S. N. Reduced Hydraulic Permeability of Three-Dimensional Collagen Scaffolds Attenuates Gel Contraction and Promotes the Growth and Differentiation of Mesenchymal Stem Cells. *Acta Biomater.* **2010**, *6*, 3978–3987.

(20) Muthusubramaniam, L.; Peng, L.; Zaitseva, T.; Paukshto, M.; Martin, G. R.; Desai, T. A. Collagen Fibril Diameter and Alignment Promote the Quiescent Keratocyte Phenotype. *J. Biomed. Mater. Res. - Part A* **2012**, *100 A*, 613–621.

(21) Li, L.; Hu, H.; Larson, R. G. DNA Molecular Configurations in Flows near Adsorbing and Nonadsorbing Surfaces. *Rheol. Acta* **2004**, *44*, 38–46.

(22) Smith, D. E.; Babcock, H. P.; Chu, S. Single-Polymer Dynamics in Steady Shear Flow. *Science* **1999**, *283*, 1724–1727.

(23) Claire, K.; Pecora, R.; V, S. U. Translational and Rotational Dynamics of Collagen in Dilute Solution. *J.of Phys. Chem. B* **1997**, *5647*, 746–753.

(24) Chung, W.-J.; Oh, J.-W.; Kwak, K.; Lee, B. Y.; Meyer, J.; Wang, E.; Hexemer, A.; Lee, S.-W. Biomimetic Self-Templating Supramolecular Structures. *Nature* **2011**, *478*, 364–368.

(25) Saeidi, N.; Karmelek, K. P.; Paten, J. A.; Zareian, R.; DiMasi, E.; Ruberti, J. W. Molecular Crowding of Collagen: A Pathway to Produce Highly-Organized Collagenous Structures. *Biomaterials* **2012**, *33*, 7366–7374.

(26) Rudisill, S. G.; DiVito, M. D.; Hubel, A.; Stein, A. In Vitro Collagen Fibril Alignment via Incorporation of Nanocrystalline Cellulose. *Acta Biomater.* **2015**, *12*, 122–128.

(27) Hayes, S.; Lewis, P.; Islam, M. M.; Doutch, J.; Sorensen, T.; White, T.; Griffith, M.; Meek, K. M. The Structural and Optical Properties of Type III Human Collagen Biosynthetic Corneal Substitutes. *Acta Biomater.* **2015**, *25*, 121–130.

(28) Gathercole, L. J.; Barnard, K.; Atkins, E. D. T. Molecular Organization of Type IV Collagen: Polymer Liquid Crystal-like Aspects. *Int. J. Biol. Macromol.* **1989**, *11*, 335–338.

(29) Brown, A. I.; Kreplak, L.; Rutenberg, A. D. An Equilibrium Double-Twist Model for the Radial Structure of Collagen Fibrils. *Soft Matter* **2014**, *10*, 8500–8511.

83x48mm (150 x 150 DPI)